DRA/HQ

FINAL REPORT: RESEARCH STUDY OF SPACE PLASMA BOUNDARY PROCESSES

Principal Investigator: E. W. Greenstadt
Co-Investigator: W. W. L. Taylor

(NASA-CR-174351) RESEARCH STUDY OF SPACE PLASMA BOUNDARY PROCESSES Final Report, 1 Oct. 1983 - 30 Sep. 1984 (TRW Space Technology Labs.) 45 p HC A03/MF A01 CSCL 20I G3/75

N85-19823

Unclas 14206

Period of Performance:

1 October 1983 through 30 September 1984
(third year of study period)

Prepared for

NASA Headquarters
Washington, D.C. 20546

October 23, 1984

Applied Technology Division
Bldg. R1, Room 1176
TRW Space and Technology Group
One Space Park
Redondo Beach, California 90278
(213) 536-2015

TABLE OF CONTENTS

FINAL REPORT: RESEARCH STUDY OF SPACE PLASMA BOUNDARY PROCESSES

Principal Investigator: E. W. Greenstadt

Co-Investigator: W. W. L. Taylor

1. INTRODUCTION

This is the final report of the third year of an investigation into the feasibility and development of computer graphic representations of plasma boundaries in space. It is not unreasonable to declare the project a success, especially in view of the evolving goals the project itself has fostered. We started out to develop three-dimensional conceptualizations of plasma processes in and around the magnetosphere as an aid to our ongoing research efforts, and wound up making animated films of the bow shock in the solar wind. Although the animation objective and the animation itself are supported separately by TRW's IR & D funds, we have found it necessary to devise our conceptualizations with animation in mind, because the physics we want to use our graphics for requires an understanding of the variability of space plasma processes. This variability is difficult to comprehend just by comparing static "spacescapes" and reconstructing their evolution mentally. Given this diversion, or expansion, of purpose, we are well on our way toward developing the techniques of computer-graphic sketching of plasma processes in a way that has greater potential than we originally anticipated.

The following sections describe the objectives and history of the project and the progress of this year's program. We close with our recommendations for

further work.

2. OBJECTIVES

The general objective of this project is to develop symbolic representations, in three dimensional computer-generated images, of plasma boundaries and processes in the Earth's magnetosphere and in the interaction region between the magnetosphere and the solar wind. The purpose of such images is to promote rapid comprehension of complicated relationships among various elements of the Earth's plasma environment that can be obtained only by visual means. We are interested in the gases, wakes, electromagnetic fields, shocks, and magnetohydrodynamic (MHD) waves that are present everywhere in space: How they should be visualized; how diverse data needed for a comprehensive description of space plasma phenomena can be gathered, correlated, and presented.

Our specific objective has been the creation of forms for representing the bow shock and magnetopause and their geometrically determined macrostructure on both large and small scales, and, with emphasis, the utilization of such forms as research tools. We are expressly concerned with both the composition of the images and the physics underlying them. Shock physics in particular, is enjoying a period of rapidly improving understanding, so that a significant part of this project is devoted to studying and deriving some of the current results whose properties we wish to represent.

3. HISTORY

This project began some years ago with an attempt to represent the global distribution of quasi-perpendicular and quasi-parallel structures of the Earth's bow shock. The original intent was simply to generate a persuasive picture of the shock's nonuniformity, to encourage other investigators not to overemphasize the nominal solar ecliptic plane cross section at the expense of the three-

dimensional nature of the shock. By the time we had developed a respectable computer sketch, the need for it had largely subsided, but another problem emerged. There seemed to be a serious need to emphasize the constant change in the nonuniformity caused by solar wind variation. The variation was appreciated, but our own computer sketches of the global distributions of shock structure convinced us that no one, including us, understood, or was capable of imagining, how imposing the complexity of the shock would be when literally *seen* as a dynamic responder to solar wind variation. We conceived the notion of animating the shock, and by straightforward extrapolation, the magnetopause and any other surface, boundary, or process in the Earth's plasma environment too complicated to envision statically, let alone dynamically, without visual assistance.

The key to successful depiction, in three-dimensional renderings, of tha plasma phenomena in which we are interested is the choice of computer-generated symbols that evoke rapid recognition of boundaries and other elements when viewed by an informed colleague with a minimum of explanation. The selection, coding, and perfection of such symbols is the task we set for ourselves in this project; the animation itself is supported principally by a TRW IR & D Program. We began with a desktop computer operating a four color pen plotter, programmed in Basic, and progressed to a VAX/11-750 controlling an Evans & Sutherland vector graphic, color workstation, programmed in "C". Our symbolic selections have been revised and improved to accomodate each new process, conception, and system as we've advanced.

4. STATUS ON 1 SEPTEMBER 1983

We had succeeded in completely redesigning our three-dimensional symbolism for the bow shock and its global geometric division. The redesigned visual model had been reprogrammed in "C"-language for a VAX/UNIX system operating an Evans and Sutherland (E & S) graphics console, and the program had

been tested and debugged. The new symbolism was chosen to (a) minimize Moiré patterns in the shock representation, (b) take advantage of the color pallette of the E & S system, (c) enable the depiction of the shock at higher sampling resolution than had previously been employed, (d) speed up considerably the process of generating each image, and (e) facilitate the use of images for animation (details in Annual Report, November 1983).

5. PROGRESS SINCE 1 SEPTEMBER 1983

A. *Graphic Development*. Based on the conviction that computer-animated modeling of space plasma objects and processes is the inevitable technique of future data analysis, we added to our conceptualizations of the bow shock the requirement that graphic symbolism be suitable for representation of not only static, but dynamic, conditions as well. That is, computer-created images of space plasma processes, which change as the input plasma conditions vary with time, must be composed of symbolic elements that lend themselves to incremental changes from image to image so that rapid viewing of image sequences presents the appearance of continuous, or at least smooth, physical variation. We proceeded with this requirement in mind.

Two data sets were selected from ISEE-1 and ISEE-3 magnetometer and plasma records. These sets appeared adequate to test the new symbolism's clarity and its suitability for animation, and at the same time to test some of the assumptions underlying both the shock model itself and the way we presently conceive of letting the variable solar wind modify it. One data set was the same one used for our first, cruder attempt at animation last year, which demonstrated well the need for a dynamic requirement separate from those for successful static representations. This first set covers a two-and-a-half-hour interval of ISEE-3 data in which the IMF varied radically and continually from its average stream angle; the set ideally illustrates the global changes of q-perp/q-par.

pattern on the shock that can occur, and how much the real shock can differ from the "typical" shock customarily used for presenting or visualizing results.

The second set covers a one-hour interval in which ISEE-1 was subject to repeated crossings of the bow shock, some of which appeared to represent q-perpendicular and some q-parallel structures. The IMF, measured independently upstream by ISEE-3 at eight times the sampling rate of the first case, showed, in contrast to the first case, only small variation about an average direction not far from the average stream angle.

An animation film (and videotape) was made, supported by TRW's IR & D funds, for each data set described above. In the second case, the location of ISEE-1 at the shock was represented by an asterisk that was made to blink on and off when the local structure was q-parallel at ISEE-1 and to change color between white and red, depending on whether ISEE-1 was outside or inside the bow shock. Thus the ISEE-3 solar wind data, which were used to define graphically the bow shock's position and structural distribution, became a "predictor" of what local conditions were to be expected at ISEE-1, and the latter became a "tester" of the predictions and hence of the assumptions underlying them. The assumptions included:

1. The uniformity of the solar wind and IMF over the distance from ISEE-3 to ISEE-1;

2. The delay time from ISEE-3 to ISEE-1;

3. The model for global shock scaling of magnetopause and shock standoff distances (from earth);

4. The bow shock's shape;

5. The criterion for q-perpendicular/q-parallel separation (we used $\vartheta_{Bn} = 45°$);

6. The arrival directions of solar wind plasma and IMF variations (we took both to be directly along V_{SW}).

The three attached color Figures 1, 2, 3 illustrate the images we are

currently using and show our capability for arbitrary zoom and viewpoint selection. Figure 4 displays the configuration of the spacecraft and the shock and solar wind assumptions used in constructing each image from a sequence of parallel "slabs".

The animation test was reasonably successful in general. The predicted q-perp/q-par. division was located close to ISEE-1, as the latter's data demanded, but not close enough to cross the spacecraft whenever it should have. Similarly, the average shock envelope did not cross ISEE-1 out- or inbound exactly as predicted. This discrepancy seemed to be correctable by adjusting the assumed delay between the two spacecraft. We are contemplating the rest of the assumptions as this is written. The most outstanding success seems to have been that our guesses about how to produce decent animation were essentially right in that the first try with the new symbolism resulted in smooth, visually acceptable image changes.

Two presentations of our graphics, in the form of animations, were made since September, the first as incidental accompaniment to a review paper, at the Napa Conference, the second as a report to the geophysical community, at the May AGU meeting in Cincinnati. The purpose of these reports has been to exhibit our technique, to display physical insights clarified by the technique, and to solicit views of other experts on numerical simulations regarding state of the art improvements applicable to our technique. The specific meetings at which presentations were made were:

> AGU Chapman Conference on Collisionless Shocks in the Heliosphere; "Oblique, parallel, and quasi-parallel morphology" by E. W. Greenstadt (Invited review), Napa, 20-24 February, 1984.
>
> AGU Spring Meeting; "Animated simulation of global bow shock structure" by E. W. Greenstadt and K. F. Yee (Poster session on Numerical simulation of space plasmas), Cincinnati, 14-17 May, 1984.

B. *Physical Processes*. Having satisfied ourselves that the new symbolic representations of the bow shock were suitable to animation with the E & S format, we turned our attention to expanding the inventory of plasma phenomena we can simulate. We engaged in numerous activities, supported in part by other funded programs, to keep current and active in the physics of space plasmas. One important result has just emerged from this part of our effort. We have demonstrated clearly that the earth's bow shock must include a region in which quasi-perpendicular and quasi-parallel structures coexist locally, or, more accurately, must alternate in a periodic pattern in the shock surface to form a third, "transition" section of the shock. Figure 5 shows the kind of variations of ϑ_{Bn} that occur at the shock where *average* ϑ_{Bn} is 45°, when typical foreshock waves of quite modest amplitude $\delta B/B = 0.2$ or 0.4 (b/B in the figure) are convected to it by a typical solar wind.

Instantaneous ϑ_{Bn} differs from its average for appreciable intervals of time and surface distance. One report describing the result and some of its consequences has just been finished and submitted for publication; a draft of this paper is attached as Appendix 1. The result described in Appendix 1 will necessarily have a major impact on the construction of bow shock images and on foreshock images we plan to construct in the future. We are preparing a second draft report describing an important consequence of the foregoing result, epecially for computer graphic sketches, namely that the conventional depiction of the bow shock, and therefore the magnetosheath and foreshock as well, as two mutually exclusive quasi-perpendicular and quasi-parallel sections must be modified to include the transition sections too. If we are interested in the quasi-parallel structure, we must now ask what part of the shock will fit in this category regardless of the presence of large amplitude waves with their changes in ϑ_{Bn} . That is, what part of the shock is *always* quasi-parallel, even when the

local waves impose a maximal excursion on ϑ_{Bn}.

Figure 6 shows two subareas of the shock, viewed from the sun's direction as projected on the y-z plane. The circle at the center marks the outline of the shock in the y-z plane (at x = 0); the large area still open at the left edge of the figure, is the region where the shock structure should be q-parallel in the presence of waves of relative amplitude $\delta B/B = 0.5$. The smaller oval encloses the region where the shock should be q-parallel even in tha presence of waves of relative amplitude $\delta B/B = 0.8$. We assume in drawing these sketches that the average field is at the 45° stream angle. The important message here is that the *true* q-parallel part of the shock occupies a great deal less than the left half that might naively have been imagined.

We believe the areas defined above are at best approximate in that, strictly speaking, ϑ_{Bn} is not the best criterion for dividing regions. The areas were derived by finding the loci where $\vartheta_{Bn} \leq 45°$ at the maximal excursion of waves of the respective amplitudes. Aside from the issue of whether 45° is an accurate discriminator of shock structure, the correct angle should not be that between **B** and the three-dimensional normal to the shock, **n**, but that between **B** and the normal $\mathbf{n}_c$ to the intersection C of the shock with the plane containing **B** and the x-axis. As **B** changes with the wave, so also does the **B**-**x** plane and $\mathbf{n}_c$. The loci enclosing the invariant q-parallel structure taking into account this effect, defined by $\vartheta_{Bnc} = \arccos(\mathbf{B}(t) \cdot \mathbf{n}_c(t))$, are much more complicated to derive than the simple ones illustrated in Fig. 6, and have not yet been worked out.

The addition of further details to images of the bow shock will be of little value unless the transition area is included. More importantly, the graphic characterization of downstream regions, such as the part of the magnetosphere affected by q-parallel structure transmitted through the magnetosheath, will have to be carefully delineated with subregions of the shock in mind.

C. *Other Activities*. Mr. Greenstadt served as Editor of the chapter produced by the Working Group 10, which he chaired, at the Solar Terrestrial Physics Workshop in Coolfont, West Virginia, last year (see below). He also serves as a member of the Data Systems Users Working Group (DSUWG). Dr. Taylor has continued as a member of the DSUWG, and contributes directly to our constant efforts to keep abreast of technological developments in computer data reduction, analysis, and networking, and to acquire and apply new equipment to this project whenever possible.

D. *Reports*. Two presentations including graphics results were listed above. Written reports, prepared or published are as follows:

"Scale lengths in quasi-parallel shocks", by J. D. Scudder, L. F. Burlaga, and E. W. Greenstadt, J. Geophys. Res., 89, 7545, 1984.

"The structure of oblique subcritical bow shocks: ISEE 1 and 2 observations", by M. M. Mellott and E. W. Greenstadt, J. Geophys. Res., 89, 2151-2161, 1984.

"Collisionless shock waves in the solar terrestrial environment", Chapter 10, E. W. Greenstadt, ed., in "Solar Terrestrial Physics: Present and Future", D. M. Butler, and K. Papadopoulos, eds., NASA Reference Publication 1120, 1984.

"Oblique, parallel, and quasi-parallel morphology of collisionless shocks", by E. W. Greenstadt, in "Collisionless Shock Waves in the Heliosphere", B. Tsurutani and R. Stone, eds., in preparation for the Am. Geophys. Union, 1984.

"Variable ϑ_{Bn} in the shock-foreshock boundary observed by ISEE-1 and -2", by E. W. Greenstadt and M. M. Mellott, submitted to J. Geophys. Res., 1984.

Cover pages of the foregoing papers are reproduced in Appendix 2, except for the last, which is attached in its entirety as Appendix 1.

6. SUMMARY

Vector, computer graphic representations of the global distributions of bow shock structures, and elementary animation of the dynamics of those distributions in the changing solar wind, for selected cases, now exist as results of this

project. The programming tools and codes developed for these results are adaptable to other cases and can be applied in a rudimentary way to other features of the plasma environment.

7. RECOMMENDATIONS

We can make several recommendations independent of continuation of this particular project. First, we are convinced that our objective, computer graphic representations of space physical processes, is a desirable, viable, and productive goal. Real-time animation, although distant, is even more to be desired, so that representations suitable to animation should be part of computer graphic development.

Second, speed of image production is not currently adequate for real-time animation. Assembly, or development, of equipment capable of higher graphic calculation and production rates should be supported. However, development of appropriate symbolic representations can be carried out separately, as long as attention is given to creating images likely to be independent of particular hardware and software solutions to the speed problem.

Third, computer graphic representations should be developed for a wider assortment of space plasma phenomena than has been dealt with so far. We would expect new problems to arise that have not yet appeared in our work.

Finally, computer techniques should be expanded to include, or incorporate, raster graphic figures with color fill symbols, hidden line removal for vector graphic sketches, and shading algorithms for raster sketches. These methods all involve foreseeable problems of one kind or another. For example, hidden line removal slows down vector image generation considerably. There will be unforeseen problems as well. We do not therefore underestimate the effort needed to bring these techniques under usable control, but we think it will

result in a valuable approach to data analysis. At the moment we favor as an initial expansion an attempt to blend vector and raster elements into composite pictures that will get around some of the problems we envision without adding too serious a burden of number crunching.

We recommend broad support for the application of computer graphic development to space plasma data analysis, taking into account all the above observations. We believe, however, that the fundamentals of animation have been sufficiently advanced to justify returning the focus of attention to the problem of three-dimensional representations of a diversity of magnetospheric phenomena. Thus, we also have recommendations for specific tasks related to our own original approach:

Q-Perpendicular/Q-Parallel Transition. As already noted, recent calculations suggest that a substantial region of transition exists separating purely q-perp from purely q-par sections of the bow shock (Appendix 1 and Fig. 6) above). This region should be characterized by locally periodic, or nearly periodic, alternation between the two structures, because of large-amplitude waves impinging on the shock from upstream. We believe a representation of this additional region must now be incorporated in any graphic shock model.

Foreshock. The foreshock as an implicit substructure of the q-parallel, collisionless shock, so that no depiction of the shock is truly complete without a foreshock element. At the Napa shock conference, Scudder introduced a three-dimensional graphic representation of foreshock boundaries extending like visors into the upstream region from the bow shock surface. This representation should be examined carefully, modified, if necessary, and a foreshock configuration should be added to

bow shock images.

Venus. As there is reason to believe that there may be significant differences between the distributions of structural forms on the Venus and Earth bow shocks, the model we have been developing should be appropriately modified to produce images of Venus' shock.

Magnetopause. As we have noted in the past, a representation of the magnetopause has already been included in our graphic programs for this study. We have not, however, defined what physical distinctions we wish to make in our representations of the magnetopause surface. Noting the rapid progress being made in reconnection studies, and interest expressed by magnetospheric experts in the possible use of our techniques, other investigators should be consulted on this matter, and the adaptation of our programs to magnetopause modeling should be explored.

Volume Representations. Thus far, we have confined our model representations to surfaces only. But the physical processes in which we are interested, of course, involve whole volumes of space. We are thinking particularly of the foreshock, the magnetosheath, and the magnetosphere. We urge exploration of the more difficult problem of representing processes within these important volume elements of the space plasma environment. This is a serious challenge to computer graphics technology in general, and efforts should be expanded to include raster graphics apparatus and techniques, which we believe will be necessary to meet the challenge.

Propagation of IMF Variations. The weakest assumption underlying our

efforts to produce sequences of bow shock images governed by the flowing solar wind has been the modeling of the IMF as a series of sampled increments uniform in planes, or slabs, perpendicular to the flow direction, i. e., perpendicular to the sun-earth line. This assumption is suitable for the solar wind plasma under most circumstances, but fluctuations of the IMF are likely to propagate along the *average* IMF at least half the time, thus approaching the bow shock from a direction usually about 45° away from that of the solar wind itself. The programs we have developed should be modified to take this effect into account.

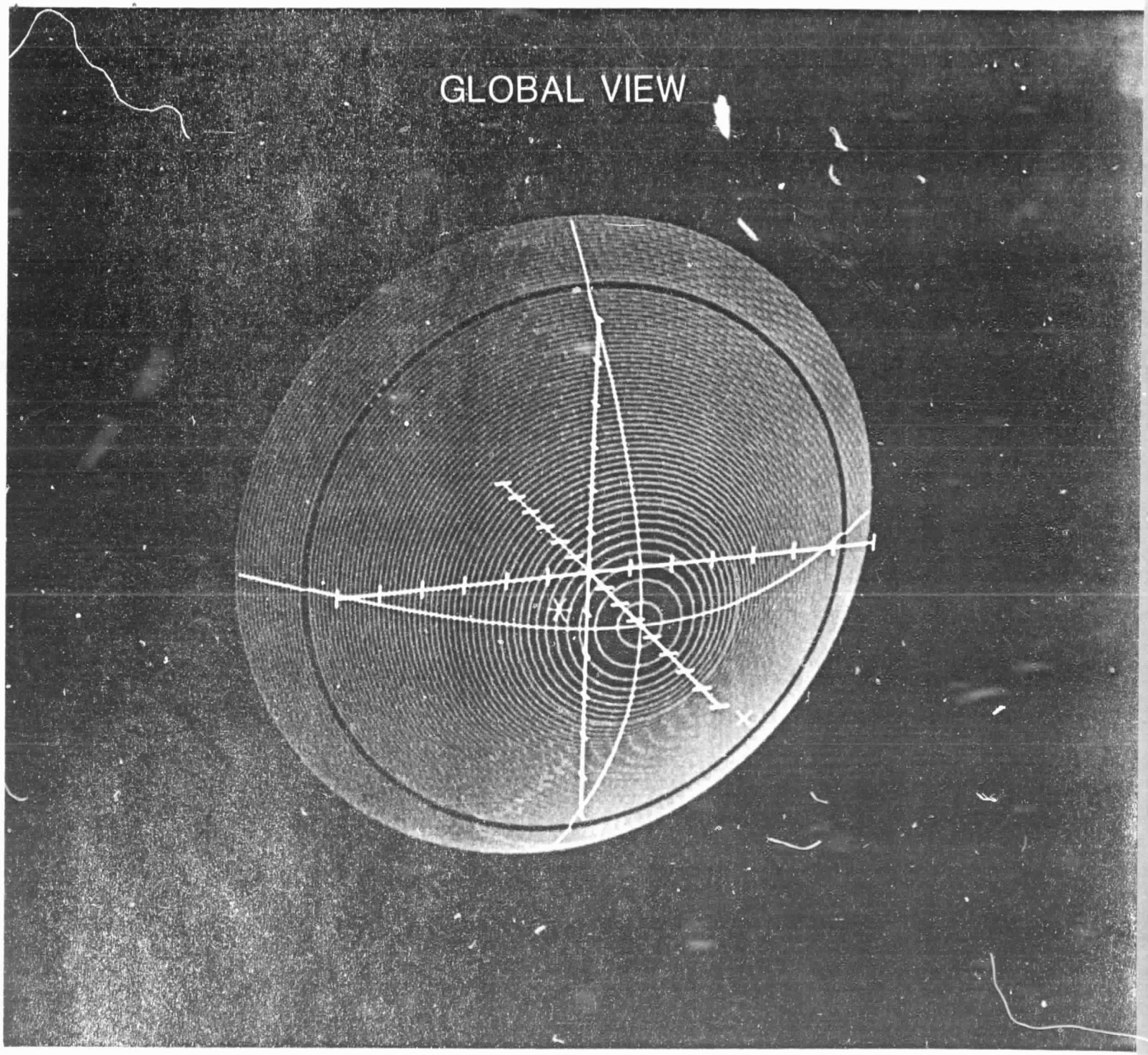

Figure 1. Earth's bow shock, with quasi-perpendicular (blue) and quasi-parallel (green) sections determined from ISEE-3 solar wind data, and ISEE-1 at asterisk position. Red asterisk means the satellite was inside the shock.

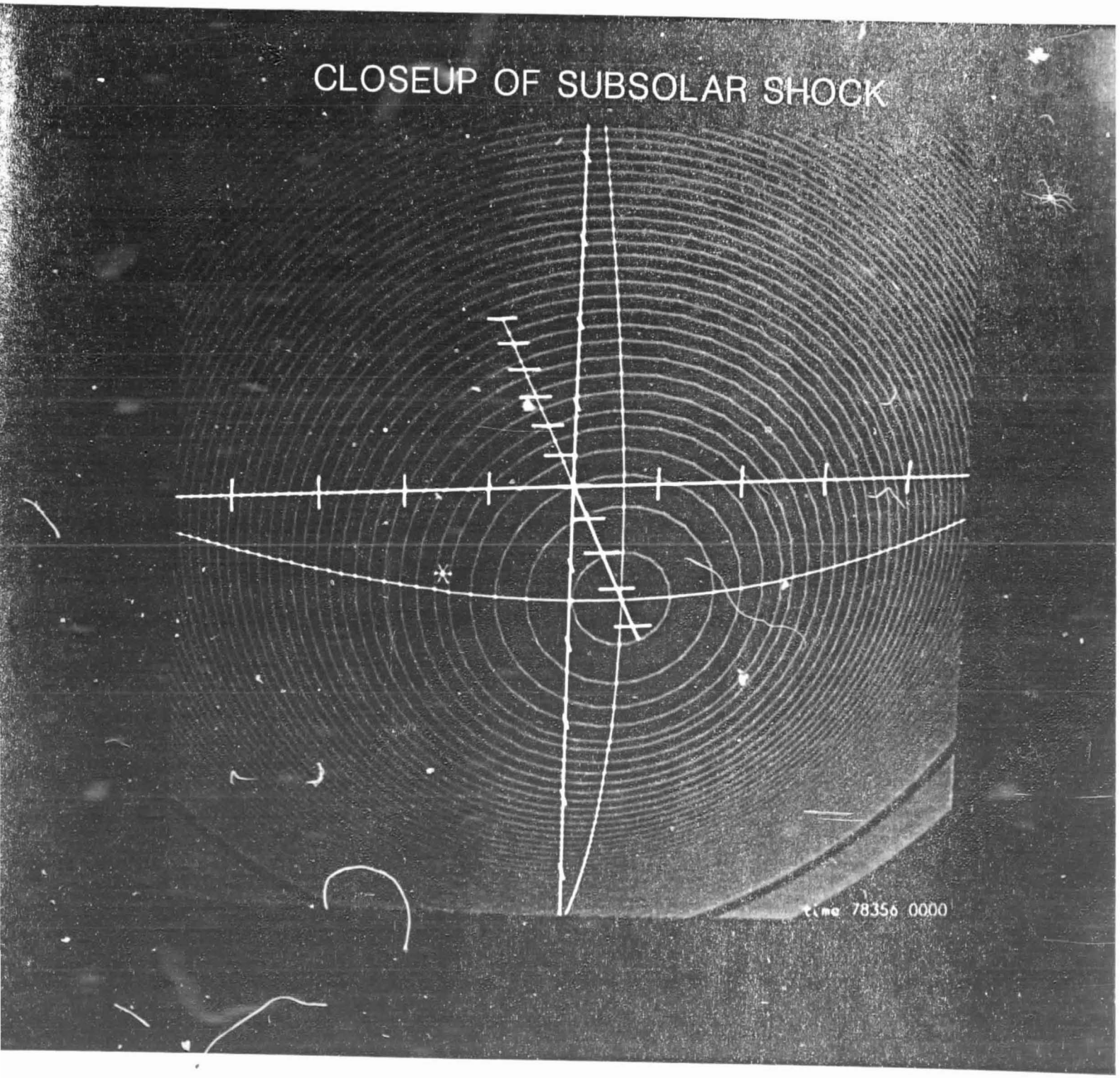

Figure 2. Zoom, i.e., magnified view of bow shock. White asterisk means the satellite was outside the shock.

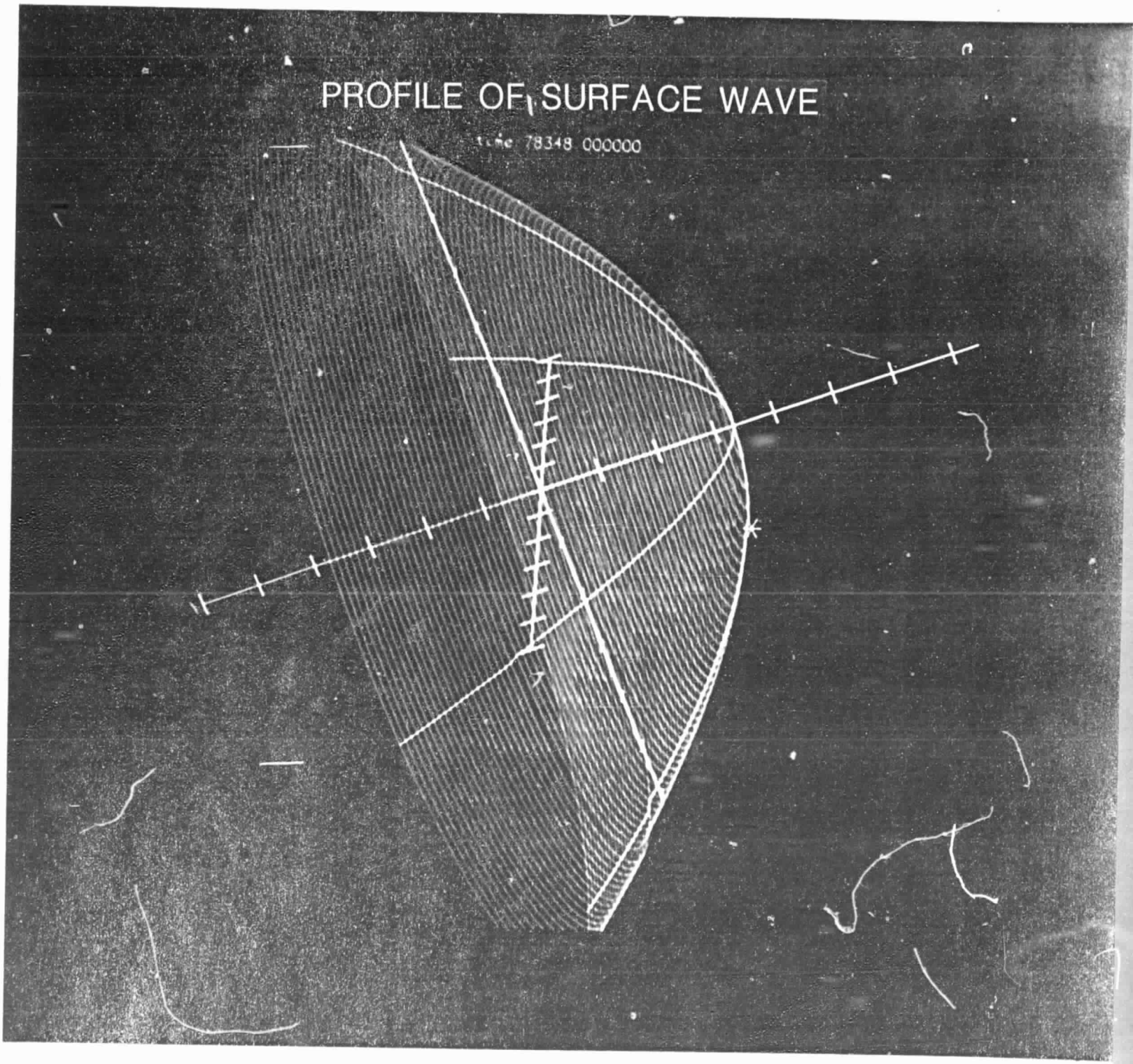

Figure 3. Side view, showing satellite outside shock after solar wind has pushed shock inward, causing travelling surface wave, visible at the edge near the bottom.

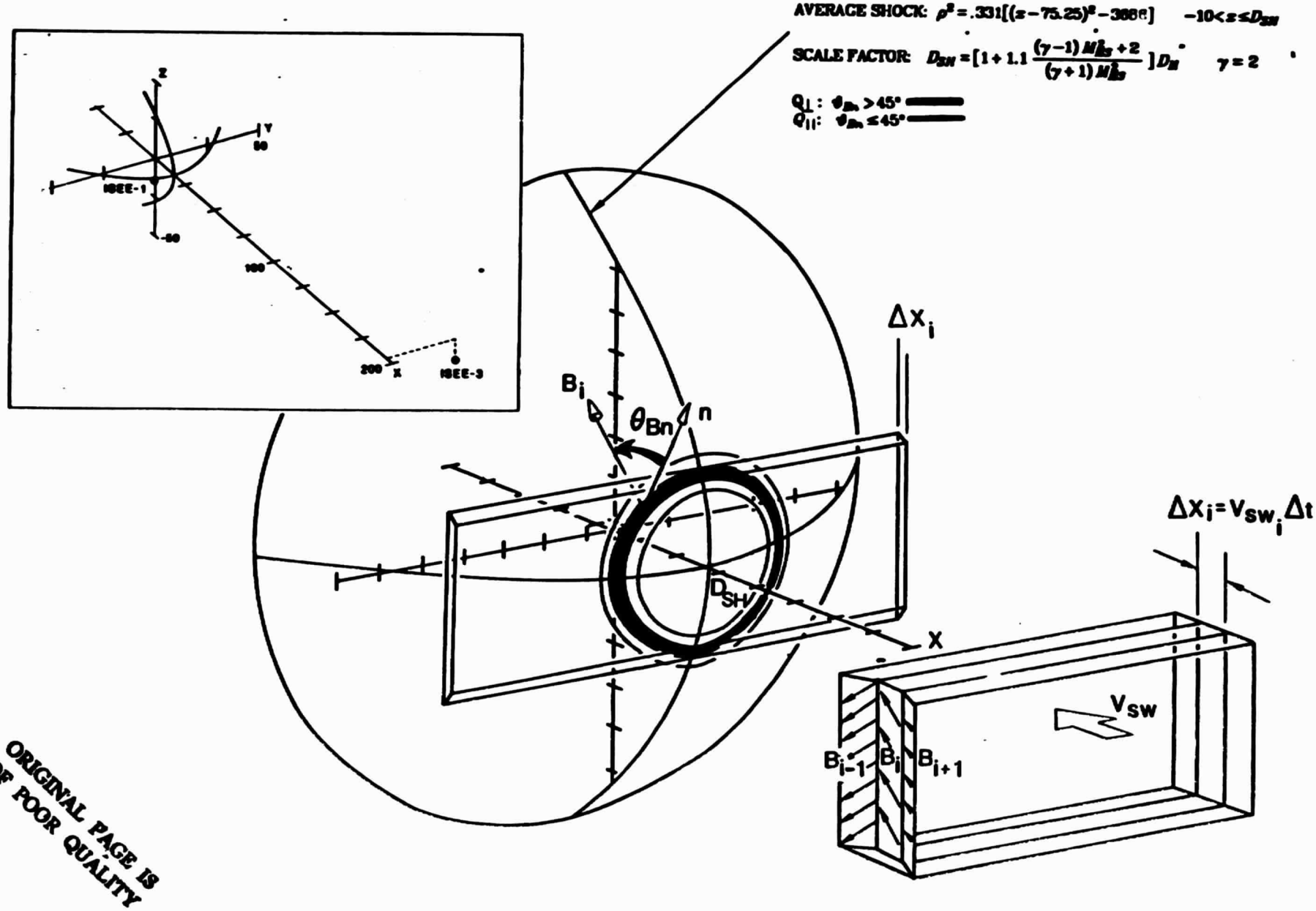

ORIGINAL PAGE IS OF POOR QUALITY

Figure 4. Shock model with sampled solar wind and IMF arriving along x-axis. Each sample defines a circular cross section of the shock which is divided into q-perpendicular and q-parallel arcs.

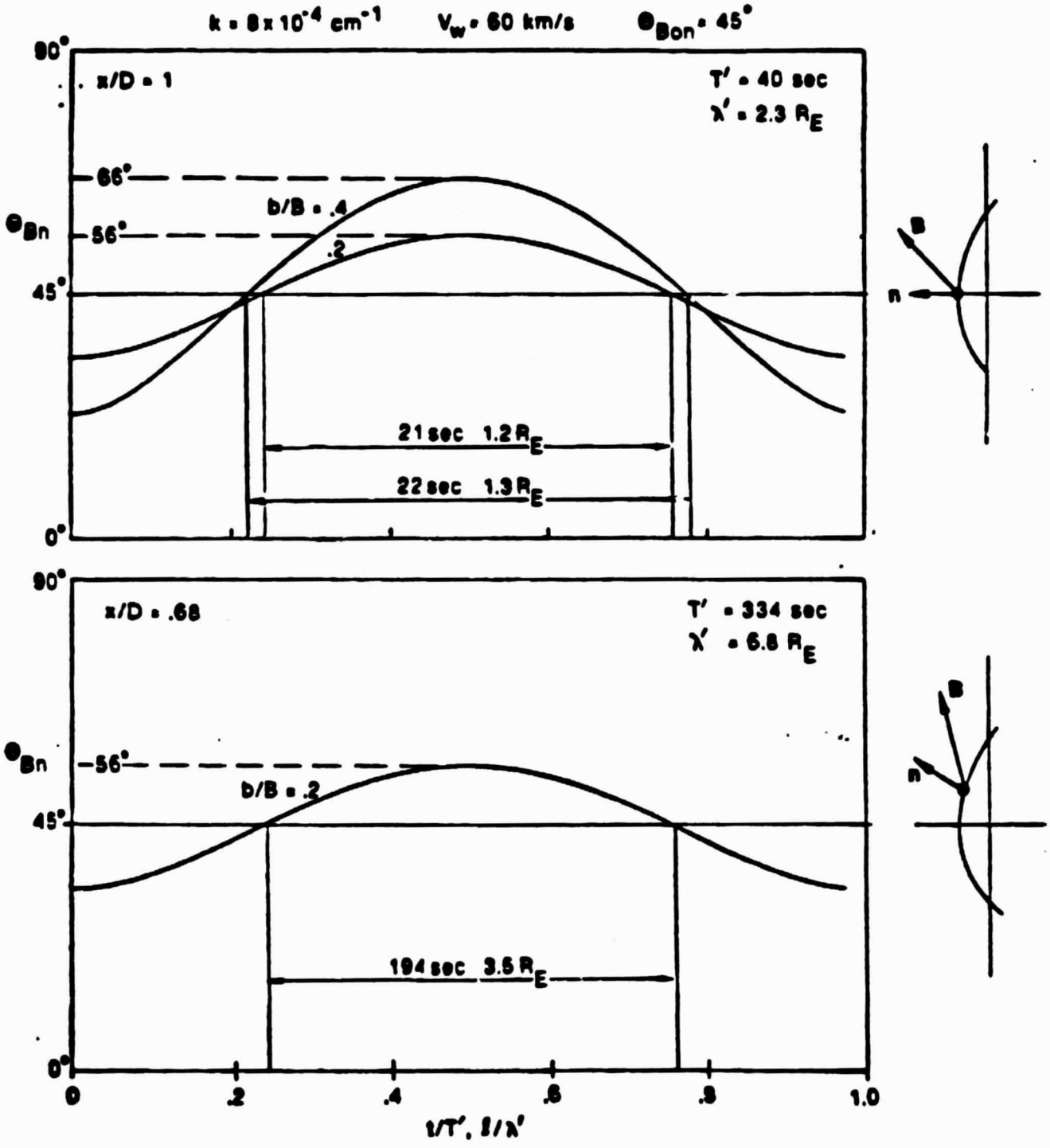

Figure 5. Computed values of the shock normal angle for typical wave and solar wind parameters at two representative locations on the bow shock (sketches at right).

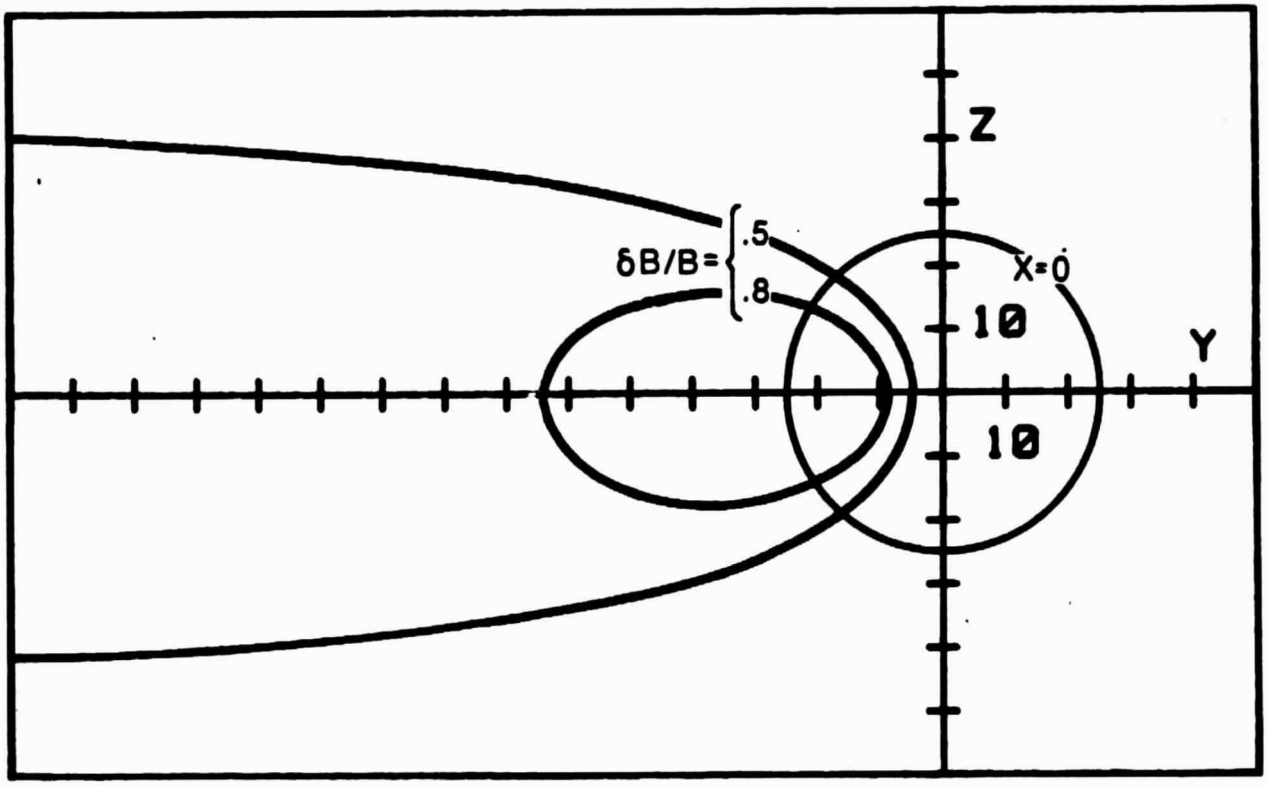

Figure 6. Anti-sunward, i.e., solar wind's, view of the bow shock projected on the y-z plane. The circle around the origin is the intersection of the hyperboloidal shock with the y-z plane (at x = 0). The two heavy curves define the projected boundaries of the regions within which the local shock structure would be expected to be q-parallel, for an IMF at the nominal stream-angle, even when waves of the respective relative amplitudes are convected to the nominal shock surface. Each tic is ten earth radii.

APPENDIX 1

NEW REPORT, SUBMITTED FOR PUBLICATION

VARIABLE ϑ_{Bn} IN THE SHOCK-FORESHOCK BOUNDARY OBSERVED BY ISEE-1 AND -2

by

E. W. Greenstadt

Space Sciences Department, TRW Inc., Redondo Beach, California

M. M. Mellott

Department of Physics and Astronomy, University of Iowa, Iowa City, Iowa

Abstract. Saturated ULF waves in the foreshock, $\delta B/B \sim 1.0$, $\omega/\Omega_p \sim 0.1$, are convected by the solar wind to the quasi-parallel shock where the *average* field-normal angle $\vartheta_{Bn} \leq 45°$. Several examples from ISEE 1 and 2 magnetometer data show waves that defined local, instantaneous ϑ_{Bn} very different periodically from the average. Local geometric conditions at the nominally quasi-parallel shock varied from nearly parallel to nearly perpendicular, at the periods of typical upstream waves. Clear magnetic shock transitions occurred when ϑ_{Bn} was temporarily quasi-perpendicular.

INTRODUCTION

One of the major controlling factors of the structure of a collisionless shock is ϑ_{Bn}, the angle between the upstream magnetic field and the local normal to the shock surface, or wave envelope. When ϑ_{Bn} is high ($90° \geq \vartheta_{Bn} \geq 60°$), the shock is quasi-perpendicular; when ϑ_{Bn} is low ($30° \geq \vartheta_{Bn} \geq 0°$), the shock is quasi-parallel [Greenstadt, 1984]. These terms denote, phenomenologically [Greenstadt and Fredricks, 1974], shocks whose magnetic signatures in the shock or spacecraft frame are characterized by abrupt, clearly defined jumps in average field over times generally on the order of less than 30 seconds (q-perpendicular) or by lengthy upstream and downstream wavetrains, sometimes difficult to distinguish, of large amplitude $\delta B/B \sim 1$ and periods of seconds to tens of seconds (q-parallel) in which the particle shock transition is embedded

[Scudder et al., 1984]. The *upstream* wavetrains define part of an extensive region ahead of the shock, called the foreshock, whose full development is a prominent feature of the q-parallel structure.

A significant part of these upstream wavetrains is expected to arise in an instability in which ions reflected from the shock interact with the solar wind [Fairfield, 1969; Barnes, 1970; Barnc et al., 1980 ; Lee, 1982; Winske and Leroy, 1984]. For need of a term, we shall say the shock is in a "transitional" condition when $\vartheta_{Bn} \sim 45°$. By this we mean that reflected ions escaping the shock upstream at $\vartheta_{Bn} < \sim 60°$ interact with solar wind to generate transverse waves which, in various stages of development, are convected back to the shock where, until ϑ_{Bn} drops to ~40°, they are reasonably distinguishable from the compressional waves and pulses that mark the true quasi-parallel shock profile. Both observation [Hoppe et al., 1981] and theory [Winske and Leroy, 1984] have shown the transverse waves develop relative amplitudes $\delta B / B_0$ at least ~0.5 in the transitional foreshock, where $\mathbf{B}_0$ is the average upstream, or solar wind, field. Recall that the angle and field variation are related by $\vartheta_{Bn} = \arccos(\mathbf{B} \cdot \mathbf{n})$, where $\mathbf{B} = \mathbf{B}(t) = \mathbf{B}_0 + \delta\mathbf{B}(t)$, $\delta\mathbf{B}(t)$ represents the wave vector, and $\mathbf{n}$ is the local normal.

In principal, ions rejected by one process or another, say, reflection or post-shock heating and scattering, can leave the shock for any $\vartheta_{B0n} < \sim 60°$ and contribute to the instability driving the upstream waves. In fact, beams must leave for a *range* of ϑ_{B0n} in order to drive the instability to saturation. The instability, and wave growth, proceed as rejected ion beams continue to be fed into the upstream interaction while the solar wind sweeps its field lines and their shock-intersections across the shock toward lower ϑ_{B0n}. The resulting waves are returned to the shock somewhere at appreciable amplitude, where the instantaneous values of ϑ_{Bn} cannot be ϑ_{B0n}, but rather some $\vartheta_{Bn}(t)$. If wavegrowth is fast enough, the possible paradox arises in which escaping particles create

waves which, when convected back to the shock, define local ϑ_{Bn} 's that periodically discourage or distort the escape of beams needed to maintain the instability, thereby modifying the above, simplified upstream process in an as yet undefined way. In applying this argument, we are thinking of ϑ_{Bn} with respect to a first order "normal" defined by some model of the global shock surface. Of course, if the local surface is itself wavy, ϑ_{Bn} (t) could be interpreted to encompass both **B**(t) and **n**(t).

Recently, Greenstadt [1984], using a *fixed* local, model normal, displayed the results of sample calculations of ϑ_{Bn} (t) indicating that the variations of ϑ_{Bn} at the shock should be expected to have significant effects on local shock structure. Figure 1 illustrates a sample calculation of ϑ_{Bn} (t) where it has been assumed that a "typical" transverse, upstream wave propagating parallel to $\mathbf{B}_0$ with k = .0008 [Hoppe and Russell, 1983] and $\delta B / B_0 = 0.5$ in a "typical" solar wind carrying a $\mathbf{B}_0$ at its "typical" stream angle (at 1 AU) encounters the shock at the subsolar point. At the subsolar point, of course, the fixed, unit normal is (1,0,0) for any model; we took our "typical" solar wind speed as 360 km/s, the wave speed as 60 km/s, and the stream angle as 45°. Such an encounter ought indeed to alter significantly the first order approximation $\vartheta_{Bn} = \vartheta_{B0n} = 45°$, and we see in the figure that ϑ_{Bn} varies between roughly 10° and 60°.

The purpose of this report is to document that such encounters are a reality: They are readily found in satellite data, in this case data from ISEE-1 and ISEE-2, and, in fact, occur at wave amplitudes considerably larger than that shown in Fig. 1.

DATA SELECTION AND TREATMENT

The cases we present here were selected by surveying four years of shock crossings by ISEE-1,2 from launch in October 1977 through December 1980. The survey was made visually with graphs of magnetic field data, from the UCLA

fluxgates [Russell, 1978], averaged every 12 seconds and plotted every four seconds. We sought well defined shocks adjacent to variable foreshock field in which the components showed higher amplitude than did the field magnitude, preferably as nearly periodic oscillations. We hoped in this manner to select largely transverse upstream waves that would permit direct comparison with simple model waves such as those of Fig. 1.

Our search yielded more than two score of potentially suitable candidate shock crossings. We show five examples in this report, three from ISEE-1, two from ISEE-2. The examples have been studied at quarter-second resolution, that is, as plots of field measurements at the sampling rate of four points per second. We use a program, more accurately a constellation of programs, developed at UCLA to plot the data and analyze them to produce filtered plots, spectral analyses, polarization hodograms, and, most importantly for this investigation, continuous computations of ϑ_{Bn}. By average ϑ_{Bn}, or ϑ_{B0n}, in this report, we mean the angle between the average $\mathbf{B}_0$ and the shock normal during four minutes of waves recorded immediately outside the shock.

EXAMPLES

Figure 2 is a full magnetic characterization of one example of the encounter of upstream ULF waves with the shock. The magnetic context can quickly be assessed by reference to the total field magnitude shown in the bottom graph of the left panel, where the shock is visible as a sharp jump near the far right of the plot. The shock was preceded by a long period wavetrain ($T <\sim 40$sec) most clearly delineated in the B_y and B_z components of the field. Other wave frequencies were obviously also present at lesser amplitudes. The character of the waves is evident in the hodograms of the two right panels and was substantially in the I-J plane-of-maximal-variance (upper right), where the superposition of the whole sequence of low-pass-filtered cycles is displayed. The wavetrain was

not exclusively transverse, but included a compressional contribution, especially near the shock. Angle ϑ_{kn} between the direction of propagation (the direction of minimal variance) and the field was about 22°, essentially, but not entirely, parallel to B_0 . The essentially transverse wave in this case had an amplitude $\delta B \sim 0.8\ B_0$. The angle ϑ_{B0n} between the average upstream B-vector and the nominal model normal was 46°.

The graph at the top of the left panel is a plot of instantaneous ϑ_{Bn} calculated from the ISEE-1 data, showing the direction of every measured field vector with respect to the local model normal, and the average $\vartheta_{B0n} \sim 46°$ as a dashed horizontal line. The dominant ULF periodicity of the waves is readily apparent in this representation, where the average period is about 38 sec. The solid curve is a plot of theoretical ϑ_{Bn} calculated for the same idealized, "typical" transverse wave as in Figure 1, but with $\delta B / B_0 = 0.8$, and for the analogous location on a nominal shock. That is, for a point at the same angle to the solar-ecliptic x-axis on a model shock scaled by the parameters we used for Fig. 1, as the point at which the data of the figure were obtained. The model we use is $\rho^2 = .04[(x-566)^2 - 304682]$, a cylindrical coordinate version of the best fit terrestrial bow shock derived by Slavin et al. [1984], where $\rho^2 = y^2 + z^2$.

Three more examples are shown in Figure 3, where we plot only the field magnitude and angle ϑ_{Bn} (t). The regularity of the oscillations of ϑ_{Bn} (t), as of the foreshock waves themselves, varied appreciably from case to case, with only the Sept. 6 case, in the middle, having waves as close to monochromatic as those of Nov. 6 (Fig. 2). In every instance, however, the difference of instantaneous ϑ_{Bn} from its average is abundantly evident. It is especially important that the value of ϑ_{Bn} at the instant of shock encounter was not necessarily anywhere near the average. Table 1 summarizes the parameters attached to the data of Figures 2, 3 and 4.

ADDITIONAL OBSERVATIONS

Although the main purpose of this report has been served by display of Figures 2 and 3, we call attention to several characteristics of the data that have appeared as a "bonus" in examining these plots and that we believe will be of considerable significance in further investigations of quasi-parallel shock structures.

First, we see that the instantaneous value of ϑ_{Bn} at the shock encounters (marked by vertical solid lines), was in every case equal to or greater than the average ϑ_{B0n} , marked in the figures. In effect, the local shock, insofar as it appeared as an abrupt, quasi-perpendicular jump in the field, always occurred while ϑ_{Bn} (t) defined temporarily a locally quasi-perpendicular geometry. Figure 4 illustrates a second very clear example, like that of the center panel of Fig. 3, where ϑ_{Bn} (t) at shock encounter was >60°, unmistakably well above ϑ_{B0n} , which was $\vartheta_{B0n} \sim 37°$ (35° in Fig. 3b).

Second, as a sort of complement to the foregoing observation, we see in three of the four cases of Figs. 2 and 3 (in all but the last) that one or two bursts of high frequency oscillations (shaded bars) occurred near the shock. These bursts took place when ϑ_{Bn} (t) was at the bottom of its cycle, i.e., when the instantaneous ϑ_{Bn} defined a temporary, unambiguous, quasi-parallel geometry. This suggests that bursts of waves associated with a locally parallel magnetic profile may have prevailed periodically when ϑ_{Bn} (t)~0°.

Third, relative elevations in the magnitude B, i.e. compressional increases in **B** in the figures, occurred during those portions of the ϑ_{Bn} (t) cycles when the angle was above the average; in other words, significant compressions occurred only when ϑ_{Bn} (t) was high, meaning the local geometry was quasi-perpendicular. The converse was not evident: not every rise of ϑ_{Bn} (t) was accompanied by a compression. The correlation has been emphasized in the figures by the vertical

dashed lines.

DISCUSSION

The graphs of Fig. 2 demonstrate that the the theoretically and empirically implied encounter of large amplitude, transverse, foreshock waves with their associated shocks at transitional average field normal angles of ~ 45° actually occurs in nature at the earth's bow shock in a pattern reminiscent of the idealized one, and that instantaneous values of ϑ_{Bn} differ radically from the average. Thus there is a definite region of the bow shock in which quasi-perpendicular and quasi-parallel geometries alternate semi-periodically; i.e., angle ϑ_{Bn} (t) may be close to either 0° or 90° at the point where the shock is forming. The character of the magnetic record in our cases suggests that the shock structure may vary locally, depending on the time variation of ϑ_{Bn} .

One further implication is that, since the high- ϑ_{Bn} sections of the wave cycles are staggered in space, the quasi-perpendicular "envelope" of the shock has an undulating surface, perhaps consistent with the one inferred from early data by Fredricks et al. [1970]. This would then imply that calculations of ϑ_{Bn} (t) should also have taken into account the compounding effect of $\mathbf{n}$(t), if a model of such variation of the normal were available. Curiously, however, abrupt shock jumps appeared at high, q-perpendicular ϑ_{Bn} *calculated from fixed* $\mathbf{n}$, thus introducing a consistency with the first order approximation that would deny the seemingly straightforward implication that a higher order calculation is needed. Resolution of these contradictory "consistencies" remains for more comprehensive investigation.

Examination of the figures encourages additional speculations. First, questions of quasi-parallel shock potential, electron potential gain, ion potential gain, and subshock formation in fully developed structures [Goodrich and Scudder, 1984; Kennel et al., 1984; Quest, 1984; Scudder et al., 1984] must be addressed

both in terms of the long magnetic scales of quasi-parallel profiles and the short scales of what appear the local, temporary quasi-perpendicular shock jumps.

Second, it takes little imagination to infer that the mixed values of ϑ_{Bn} close to the shock, accompanied as we see by mixed high and low frequency magnetic waves, are probably associated with plasma waves and with mixed distributions of upstream ions, some scattered downstream by waves further upstream, some reflected or emitted upstream from nearby q-parallel shock encounters, and some trapped in adjacent q-perpendicular shock encounters. The ion flux oscillations at typical wave periods in the foreshock described by Potter [1984] may have resulted from modulated emissions at the shock source.

We inspected one example of ion data from a quasi-parallel shock already described in the literature: Gosling et al. [1982] recorded two samples of specularly reflected ions "similar in nature to the gyrating ion beams observed within the quasi-perpendicular bow shock [Paschmann et al., 1982]". The purity of their reflection signatures in a region where diffuse distributions might have been expected, but where "no evidence for such particle debris in the contours" was noted, suggests that the signatures may have been created during a temporarily q-perpendicular, and released during a temporarily q-parallel, interval of local shock geometry.

We ran ϑ_{Bn} (t) plots for the waves surrounding the cases of Gosling et al., and found variations comparable to those illustrated in Figures 2 and 3 of this report, with the addition of considerable variations at higher frequency. The data for those cases were obtained at ISEE's highest sampling rate, so the plots were too long and too detailed to reproduce in this letter. The samples selected by Gosling et al. occurred two minutes away from the actual shock crossing, somewhat removed from the largest oscillations of the field direction. During each three-second ion sample, the direction change was relatively small, com-

somewhat removed from the largest oscillations of the field direction. During each three-second ion sample, the direction change was relatively small, compared to surrounding intervals, and the field was close to its average upstream orientation. Certainly the possibility is open that the observed ion distributions were produced elsewhere at nonaverage ϑ_{Bn} . Comprehensive investigation of ϑ_{Bn} (t), plasma, and plasma wave data in high bit rate cases, where ion distributions can be distinguished, is the obvious next step.

Acknowledgements. This study was funded by NASW-3690 and -3836 (at TRW) and NAS5-26819 (at Univ. of Iowa). The data library, processing techniques, and advice of C. T. Russell have been essential, as was the help of R. C. Elphic, L. Baum, and K. Yee in effecting the analysis. The importance of ϑ_{Bn} (t) has been espoused by C. F. Kennel for years in private discussions; its calculation was added to the UCLA data analysis programs at the suggestion of J. T. Gosling.

References

Bame, S. J., J. R. Asbridge, J. T. Gosling, G. Paschmann, and N. Sckopke, Deceleration of the solar wind upstream from the earth's bow shock and athe origin of diffuse upstream ions, *J. Geophys. Res.*, *85*, 2981, 1980.

Barnes, A., Theory of generation of bow-shock-associated hydromagnetic waves in the upstream interplanetary medium, *Cosmic Electrodyn.*, *1*, 90, 1970.

Fairfield, D. H., Bow shock associated waves observed in the far upstream interplanetary medium, *J. Geophys. Res.*, *74*, 3541, 1969.

Fredricks, R. W., G. M. Crook, C. F. Kennel, I. M. Green, F. L. Scarf, P. J. Coleman, and C. T. Russell, Ogo 5 observations of electrostatic turbulence in bow shock magnetic structures, *J. Geophys. Res.*, *19*, 3751-3768, 1970.

Goodrich, C. C., and J. D. Scudder, The adiabatic energy change of plasma electrons and the frame dependence of the cross-shock potential at collisionless magnetosonic shock waves, *J. Geophys. Res.*, *89*, 6654-6662, 1984

Gosling, J. T., M. F. Thomsen, S. J. Bame, W. C. Feldman, G. Paschmann, and N. Sckopke, Evidence for specularly reflected ions upstream from the quasi-parallel bow shock, *Geophys. Res. Lett.*, *9*, 1333, 1982.

Greenstadt, E. W., Oblique, quasi-parallel, and parallel morphology of collisionless shocks, *Collisionless Shocks in the Heliosphere, AGU Monograph*, 1984.

Greenstadt, E. W., and R. W. Fredricks, Shock systems in collisionless space plasmas, in *Solar System Plasma Physics: A Twentieth Anniversary Review*, vol. 3, edited by C. F. Kennel, L. J. Lanzerotti, and E. N. Parker, p.4, North-Holland, Amsterdam, 1979.

Hoppe, M. M., and C. T. Russell, Whistler mode wave packets in the earth's foreshock region, *Nature*, *287*, 407-420, 1980.

Hoppe, M. M., and C. T. Russell, Plasma rest frame frequencies and polarizations of the low-frequency upstream waves: ISEE 1 and 2 observations, *J. Geophys. Res.*, *88*, 2021-2028, 1983.

Hoppe, M. M., C. T. Russell, L. A. Frank, T. E. Eastman and E. W. Greenstadt, Upstream hydromagnetic waves and their association with backstreaming ion populations: ISEE 1 and ISEE 2 observations, *J. Geophys. Res.*, *86*, 4471-4492, 1981.

Kennel, C. F., J. P. Edmiston, and T. Hada, A quarter century of collisionless shock research, *Collisionless Shocks in the Heliosphere, AGU Monograph*, 1984.

Lee, M. A., Coupled hydromagnetic wave excitation and ion acceleration upstream of the earth's bow shock, *J. Geophys. Res.*, *87*, 5063, 1982.

Paschmann, G., N Sckopke, S. J. Bame, and J. T. Gosling, Observations of gyrating ions in the foot of the nearly perpendicular bow shock, *Geophys. Res. Lett.*, *9*, 881, 1982.

Potter, D. W., High time resolution characteristics of intermediate iondistributions upstream of the Earth's bow shock, in press, *J. Geophys. Res.*, 1984.

Quest, K. B., A review of simulation of quaseparallel collisionless shocks, submitted, *Collisionless Shocks in the Heliosphere*, *AGU Monograph*, 1984.

Russell, C. T., The ISEE-1 and -2 fluxgate magnetometers, *EEE Trans. Geosci. Electronics*, *GE-16*, 239-242, 1978.

Scudder, J. D., L. F. Burlaga, and E. W. Greenstadt, Scale lengths in quasi-parallel shocks, *J. Geophys. Res.*, *89*, 7545-7550, 1984.

Slavin, J. A., R. E. Holzer, J. R. Spreiter, and S. S. Stahara, Planetary Mach cones: theory and observation, *J. Geophys. Res.*, *89*, 2708-2714, 1984.

Winske, D., and M. M. Leroy, Diffuse ions produced by electromagnetic ion beam instabilities, *J. Geophys. Res.*, *89*, 2673-2688, 1984.

Table 1. Selected Characteristics of Wave Examples.

Date	ϑ_{Bn}	b/B_0	Range of ϑ_{Bn}	ϑ_{Bn} at shock	Fig. no.
22 Dec. 77	31°	0.6	3°-82°	≥55°	3a
6 Nov. 78	46°	0.8	3°-89°	~60°	2
6 Sep. 79	35°	1.0	1°-90°	~80°	3b
18 Nov. 79	41°	0.7-0.9	2°-87°	~70°	3c
25 Nov. 79	37°	0.5-0.8	0°-81°	≥65°	4

Figure Captions

Figure 1. Plot of instantaneous field-normal angle vs fraction (t/T' or l/λ') of apparent period T' or wavelength λ', in a shock or spacecraft frame stationary with respect to the solar wind, for a typical transverse foreshock wave of frequency 0.1Ω and amplitude δB/B=0.5.

Figure 2. Left, magnetic field data (lower four plots) and corresponding field-normal angle ϑ_{Bn} (irregular upper plot), vs. time for the 6 November 1978 case. A model calculation of ϑ_{Bn} for a foreshock wave of amplitude δB/B=0.5 is superposed as the smooth periodic curve in the upper panel. The solid vertical arrow marks the shock crossing. The horizontal dashed line marks the average upstream ϑ_{Bn} ;the vertical dashed lines mark the centers of compressional excursions of B; the hatched box marks a burst of high frequency oscillations close to the shock. Right, hodograms of the observed wave, showing dominant planar polarization, as assumed in the calculated behavior of the foreshock wave.

Figure 3. Three case of wave-shock encounter, showing field magnitude and ϑ_{Bn} (t) computed from the data. Symbols and lines have the same meanings as in Fig. 2.

Figure 4. A two-minute section of an additional case of shock appearance when ϑ_{Bn} was well above a relatively low, post-transitional ϑ_{B0n}.

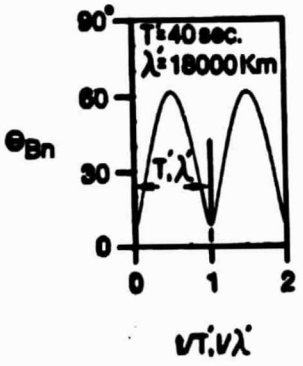

Figure 1. Plot of instantaneous field-normal angle vs fraction (t/T' or 1/λ') of apparent period T' or wavelength λ', in a shock or spacecraft frame stationary with respect to the solar wind, for a typical transverse foreshock wave of frequency 0.1Ω and amplitude bB = .5.

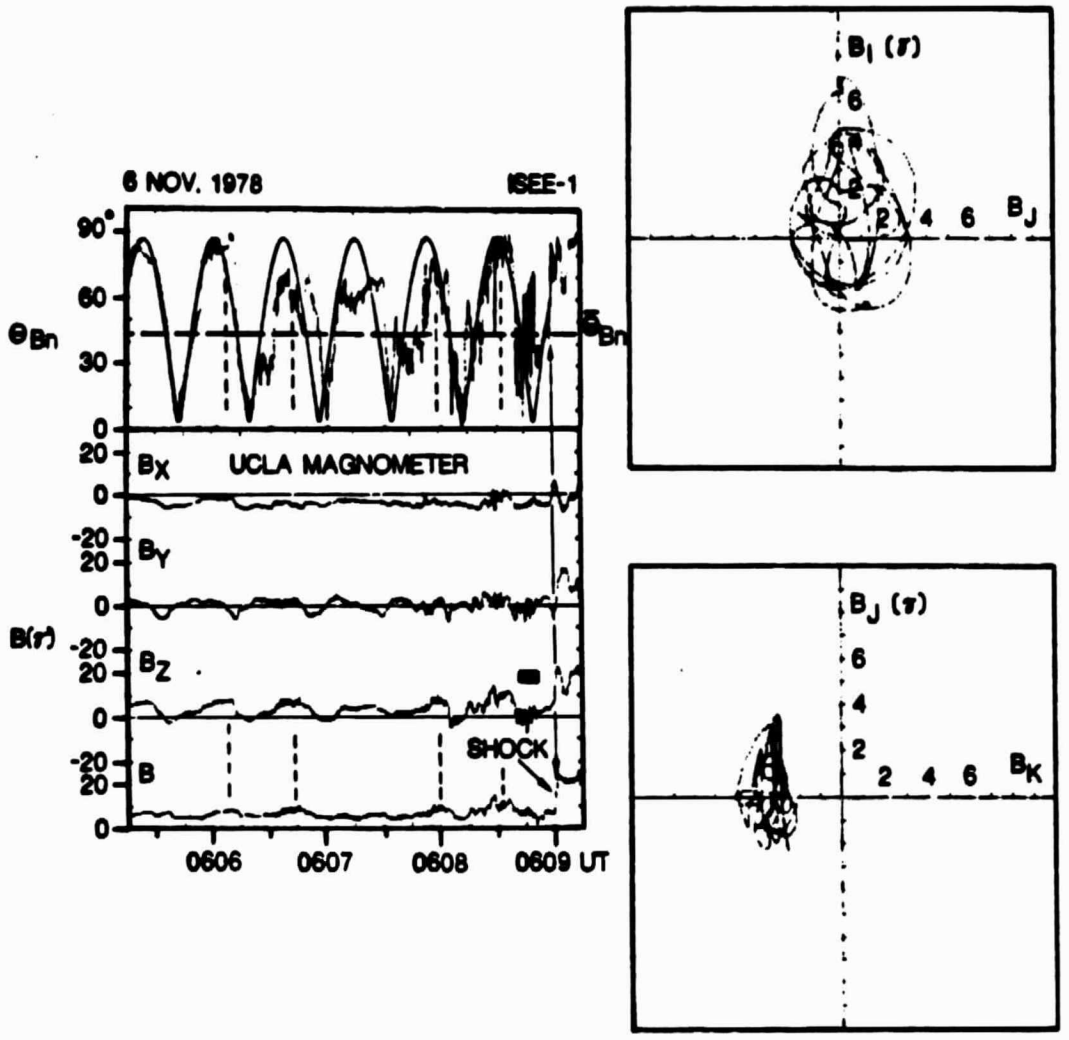

Figure 2. Left, magnetic field data (lower four plots) and corresponding field-normal angle ϑ_{Bn} (irregular upper plot), vs. time for the 6 November 1978 case. A model calculation of ϑ_{Bn} for a foreshock wave of amplitude b/B=0.8 is superposed as the smooth periodic curve in the upper panel. The solid vertical arrow marks the shock crossing. The horizontal dashed line marks the average upstream ϑ_{Bn} ;the vertical dashed lines mark the centers of compressional excursions of B; the hatched box marks a burst of high frequency oscillations close to the shock. Right, hodograms of the observed wave, showing dominant planar polarization, as assumed in the calculated behavior of the forcshock wave.

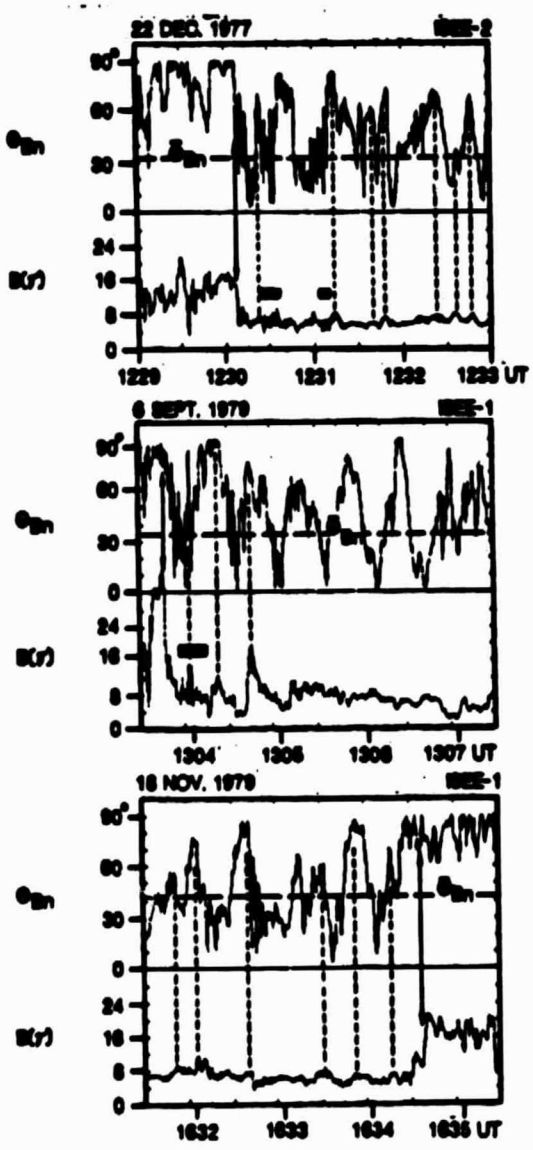

Figure 3 Three case of wave-shock encounter, showing field magnitude and ϑ_{Bn} (t) computed from the data. Symbols and lines have the same meanings as in Fig. 2.

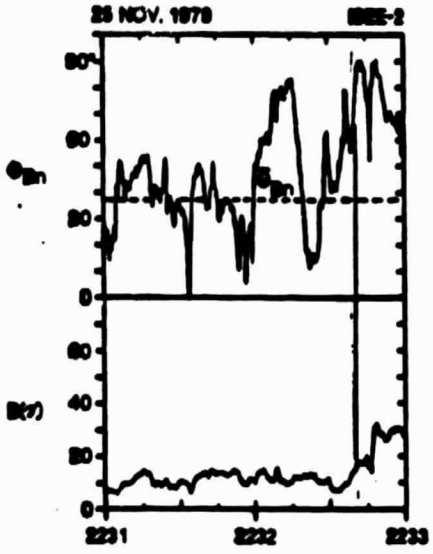

Figure 4. A two-minute section of an additional case of shock appearance when ϑ_{Bn} was well above a relatively low, post-transitional ϑ_{B0n}.

CHAPTER 10

COLLISIONLESS SHOCK WAVES IN THE SOLAR TERRESTRIAL ENVIRONMENT

JOURNAL OF GEOPHYSICAL RESEARCH, VOL. 89, NO. A9, PAGES 7545-7550, SEPTEMBER 1, 1984

Scale Lengths in Quasi-Parallel Shocks

J. D. SCUDDER AND L. F. BURLAGA

NASA Goddard Space Flight Center, Laboratory for Extraterrestrial Physics, Greenbelt, Maryland

E. W. GREENSTADT

TRW, Redondo Beach, California

Examples of an interplanetary shock and the earth's bow shock are presented to illustrate the small-scale size L_p of the fluid deceleration relative to the scale of the magnetic fluctuations, L_M, at quasi-parallel shocks. The increase in electron and ion random energies is also illustrated to occur on the short "inner" scale of L_p. The selected interplanetary and bow shock examples are both supercritical high-β shocks but have different Alfvén Mach numbers. The thickness L_p in absolute and convected Larmor radii units of the lower Alfvén Mach number interplanetary shock is larger ($\sim 10\ U'/\Omega_{ci}$) than that at the bow shock ($\sim (1\text{-}2)\ U'/\Omega_{ci}$), where U' is the plasma flow speed viewed in the normally incident shock rest frame. In both examples the scale of the fluid deceleration is much smaller than that of the up- or downstream magnetic fluctuations. The existence of steady state quasi-parallel shocks requires that the Lorentz deceleration force be much larger than the electrostatic deceleration force along the shock normal.

1. INTRODUCTION

The view of quasi-parallel shocks ($\theta_{BN} < 45°$) as broad and disordered transition regions, with scale lengths at the bow shock of several R_e, has remained uncontested in the literature for over 10 years. This characterization is largely based on the magnetometer morphology at the earth's bow shock. Recently observed interplanetary quasi-parallel shocks have also been reported to possess broad magnetic transitions with scales in excess of 10^5 km. In this paper we organize ISEE and Voyager plasma data capable of affirming or denying the "broad transition" view of such shocks by identifying the scale L_p over which the plasma decelerates across quasi-parallel shocks. We show that this deceleration scale L_p is much smaller than the spatial scale of the magnetic fluctuations, L_M, which has been previously used to characterize quasi-parallel shocks as "broad" structures. Previously, the spatially varying systematic effects in ion measurements at the standing bow shock have precluded definitive commentary on these issues.

In the framework of MHD theory a parallel shock is characterized by a discontinuous increase in temperature and a discontinuous decrease in speed in the normally incident shock frame; neither the magnitude nor the direction of the magnetic field changes [*Landau and Lifschitz*, 1960] across such a theoretically idealized shock (except for the limited regime (low beta) where a switch-on shock is possible, namely, $C_S < V_{A_x}$ and the normally incident velocity U_x bounded between $V_{A_x} < U_x < (4V_{A_x}^2 - 3C_S^2)^{1/2}$ [*Akhiezer et al.*, 1975]). Shocks in nature have a finite thickness L_p, which may be taken to be the width of the necessary transition in density or speed. Across this layer, random energy increases at the expense of the directed streaming energy. This exchange is principally initiated in quasi-perpendicular shocks by an electrostatic field E localized within this layer. Within L_p in quasi-parallel shocks there is also localized an electrostatic field, but its relative importance in the deceleration process for this class of shocks has until now not been established. In either case the distance L_E over which such an E is nonnegligible is approximately bounded by L_p. Up- and downstream of shocks, magnetic fluctuations are usually found with scale lengths L_M^+, L_M^-, where the plus superscripts refer to the low-entropy upstream regime and the minus superscripts refer to the high-entropy downstream regime. In the past the high-resolution magnetometer profiles of L_M^+ and L_M^- have been operationally used to assess the thickness of collisionless shocks, especially for those of the quasi-parallel geometry [*Cahill and Amazeen*, 1963; *Bernstein et al.*, 1964; *Greenstadt et al.*, 1970, 1977; *Auer and Völk*, 1973; *Acuña et al.*, 1981; *Tsuritani et al.*, 1983; *Kennel et al.*, 1982].

L_M^+ at the earth's bow shock is typically several R_e for a wide range of $\theta_{BN} < 45°$ [*Greenstadt and Fredericks*, 1979]. There is, however, neither experimental nor theoretical justification that the scale of the plasma deceleration L_p is necessarily synonymous with the scales of the magnetic fluctuations, L_M^+, L_M^-. The observed relative ordering of these two scales will be contrasted in this paper for the first time.

2. REGIMES OF QUASI-PARALLEL SHOCK OBSERVATIONS

Quasi-parallel shocks have until recently only been studied at the earth's standing bow shock; the first detection of an interplanetary quasi-parallel shock was reported in 1979 [*Acuña et al.*, 1981]. There is an important difference in the systematics of ion measurements which make determinations of L_p more difficult at the standing bow shock than at the propagating interplanetary shock: the plasma bulk velocity in the spacecraft frame is (is not) supersonic with respect to ion thermal speeds on both sides of a propagating interplanetary (standing bow) shock.

In order to assess the scale of the fluid speed, L_p, the speed itself must first be determined free of spatially varying systematic effects. The constituent sonic Mach number of the bulk flow in the spacecraft frame determines how much of the 4π sr of velocity space must be thoroughly sampled to allow direct model independent numerical estimates of the bulk velocity of that constituent.

The solid angle coverage in velocity space about the spatially varying local flow direction $\hat{U}(x)$ necessary for this deter-

Paper number 4A0842
0148-0227/84/004A-0842$02.00

JOURNAL OF GEOPHYSICAL RESEARCH, VOL. 89, NO. A4, PAGES 2151-2161, APRIL 1, 1984

The Structure of Oblique Subcritical Bow Shocks: ISEE 1 and 2 Observations

M. M. MELLOTT[1]

Institute of Geophysics and Planetary Physics, University of California

E. W. GREENSTADT

Space Sciences Department, TRW Space and Technology Group

We have studied the structural elements, including shock ramps and precursor wave trains, of a series of oblique low-Mach number terrestrial bow shocks. We used magnetic field data from the dual ISEE 1 and 2 spacecraft to determine the scale lengths of various elements of shock structure as well as wavelengths and wave polarizations. Bow shock structure under these conditions is essentially that of a large-amplitude damped whistler mode wave which extends upstream in the form of a precursor wave train. Shock thicknesses, which are determined by the dispersive properties of the ambient plasma, are too broad to support current-driven electrostatic waves, ruling out such turbulence as the source of dissipation in these shocks. Dissipative processes are reflected in the damping of the precursors, and dissipative scale lengths are ~200–800 km (several times greater than shock thicknesses). Precursor damping is not related to shock normal angle or Mach number, but is correlated with T_e/T_i. The source of the dissipation in the shocks does not appear to be wave-wave decay of the whistlers, for which no evidence is found. We cannot rule out the possibility of contributions to the dissipation from ion acoustic and or lower-hybrid mode turbulence, but interaction of the whistler itself with upstream electrons offers a simpler and more self-consistent explanation for the observed wave train damping.

INTRODUCTION

Study of the terrestrial bow shock is an integral part of our attempts to understand the formation of the magnetosphere and the energy transfer to it from the solar wind. Detailed examination of the shock also provides us with increased understanding of the physical processes involved in the formation of shock waves in collisionless plasmas in general. Under most conditions the bow shock is a complex and turbulent structure for which comprehensive analytic theories have only recently begun to appear [e.g., *Leroy*, 1983]. Occasionally, however, the shock loses much of its complexity and lends itself to comparison with relatively uncomplicated analytic descriptions. In this paper we describe the relatively rare but structurally simple shock which results when the solar wind is cold and has a relatively low flow velocity. For oblique shock normal angles the shocks which form under such conditions are essentially large-amplitude whistler mode waves which extend upstream in the form of phase-standing precursor wave trains.

Important early contributions to shock studies were made through investigations of the precursor wave trains, the first of which was presented by *Fairfield and Feldman* [1975]. They showed that the waves found upstream of and adjacent to low-Mach number bow shocks characteristically fell into two frequency ranges: a lower-frequency signal with periods of tens of seconds and a higher-frequency signal with periods of ~1 s. Inferred properties of the low-frequency waves matched those predicted for the whistler shock precursors. Wave polarizations, for example, changed from right handed for outward moving shocks to left handed for inward moving shocks as expected for phase-standing whistlers. Fairfield and Feldman also investigated wavelengths, although they were unable to make direct measurements of the scale lengths of the signals. They did, however, calculate the wavelengths expected for standing whistlers and inferred shock velocities using these calculated values. The inferred shock velocities were in reasonably good agreement with other estimates of shock velocities, and so the estimated wavelengths, which averaged ~500 km and ranged from 60 to 1600 km, were accepted as physically reasonable. Although these and other early observations were consistent with theory, they were all based on single-spacecraft measurements which could not establish the absolute scale of the phenomena in question. The present paper, in contrast, continues work on laminar shock structure which uses the unique capability of the ISEE 1 and 2 dual-spacecraft set to establish absolute scale lengths and intrinsic wave polarizations. Use of these data has allowed us to make detailed quantitative comparisons between shock theory and observations of naturally occurring collisionless shock waves. This analysis demonstrates that oblique low-Mach number bow shocks are indeed the predicted large-amplitude whistler waves and that the low-frequency precursors are the upstream extension of the shock structure itself.

The relation of the higher-frequency waves to shock structure is less clear. One interesting hypothesis has been that they might have been generated by decay of the standing precursors, but the properties of the high-frequency waves observed upstream of low-Mach number ISEE shocks are not consistent with those expected for products of decay of the standing whistlers. On the other hand, similar higher-frequency waves had been observed upstream of higher Mach number shocks [*Fairfield*, 1974], and it has alternatively been suggested that the higher-frequency waves seen upstream of low-Mach number shocks are merely further examples of this more general phenomenon. We will show, however, that it is unlikely that the higher-frequency waves observed upstream of low Mach number shocks are generated by the same mechanism which drives the waves observed upstream of stronger shocks.

Low-β low Mach number shocks have traditionally been designated "laminar shocks," a term first applied in theoretical

[1] Now at Department of Physics and Astronomy, University of Iowa

Paper number 3A1988
0148-0227/84/003A-1988$05.00

CHAPTER 10

COLLISIONLESS SHOCK WAVES IN THE SOLAR TERRESTRIAL ENVIRONMENT

WORKING GROUP MEMBERS

E. Greenstadt, Chairman
TRW

V. Formisano
I.F.S.I/CNR

C. Goodrich
University of Maryland

J. T. Gosling
Los Alamos National Laboratory

M. Lee
University of New Hampshire

M. Leroy
DESPA Observatorie de Meudon

M. Mellott
University of California

K. Quest
Los Alamos National Laboratory

A. E. Robson
Naval Research Laboratory

P. Rodriguez
Naval Research Laboratory

J. Scudder
NASA/Goddard Space Flight Center

J. Slavin
Jet Propulsion Laboratory

M. Thomsen
Los Alamos National Laboratory

D. Winske
Los Alamos National Laboratory

C. S. Wu
University of Maryland

CHAPTER 10

COLLISIONLESS SHOCK WAVES IN THE SOLAR TERRESTRIAL ENVIRONMENT

TRW Tech. Report No. 40789-6007-UT-00

OBLIQUE, PARALLEL, AND QUASI-PARALLEL MORPHOLOGY OF COLLISIONLESS SHOCKS

A Review for
AGU Chapman Conference on
Collisionless Shock Waves in the Heliosphere

Revised September 10, 1984

by

Eugene W. Greenstadt
Space Sciences Department
TRW Space and Technology Group
Advanced Products Laboratory
Applied Technology Division
One Space Park
Redondo Beach, CA 90278

OBLIQUE, PARALLEL, AND QUASI-PARALLEL MORPHOLOGY OF COLLISIONLESS SHOCKS

ABSTRACT

Although many of the features of natural shocks in space had been known or surmised some years ago, neither theoreticians nor laboratory experimenters had quite assembled all the idealized elements into a correct prediction of extraterrestrial observations. Shocks were classified as perpendicular, oblique, and parallel before high-quality measurements became available. Thus, some nonperpendicular profiles have appeared puzzling and unexpected. Are nonperpendicular, oblique shocks disguised in the bow shock system by its finite radius of curvature? The latest research results indicate otherwise; that is, the quasi-perpendicular/quasi-parallel division is real and intrinsic, although some characteristics may be parameter dependent. An attempt is made to summarize observational results on nonperpendicular shocks with the aim of understanding the shock as an interactive structure dependent on the geometry of shock propagation. An elementary suggestion is presented that may provide a foundation for reconciling some seemingly complicated or contradictory quasi-parallel features.